J Physiol 588.8 (2010) pp 1251–1268

The Journal of Physiology

Distinct activities of GABA agonists at synaptic- and extrasynaptic-type $GABA_A$ receptors

Martin Mortensen[1], Bjarke Ebert[2], Keith Wafford[3] and Trevor G. Smart[1]

[1] *Department of Neuroscience, Physiology and Pharmacology, University College London, Gower Street, London WC1E 6BT, UK*
[2] *Department of Molecular Pharmacology, H. Lundbeck A/S, Otilliavej 8, 2500 Valby, Copenhagen, Denmark*
[3] *Lilly UK, Erl Wood Manor, Windlesham, Surrey GU20 6PH, UK*

The activation characteristics of synaptic and extrasynaptic $GABA_A$ receptors are important for shaping the profile of phasic and tonic inhibition in the central nervous system, which will critically impact on the activity of neuronal networks. Here, we study in isolation the activity of three agonists, GABA, muscimol and 4,5,6,7-tetrahydoisoxazolo[5,4-c]pyridin-3(2*H*)-one (THIP), to further understand the activation profiles of $\alpha1\beta3\gamma2$, $\alpha4\beta3\gamma2$ and $\alpha4\beta3\delta$ receptors that typify synaptic- and extrasynaptic-type receptors expressed in the hippocampus and thalamus. The agonists display an order of potency that is invariant between the three receptors, which is reliant mostly on the agonist dissociation constant. At δ subunit-containing extrasynaptic-type $GABA_A$ receptors, both THIP and muscimol additionally exhibited, to different degrees, superagonist behaviour. By comparing whole-cell and single channel currents induced by the agonists, we provide a molecular explanation for their different activation profiles. For THIP at high concentrations, the unusual superagonist behaviour on $\alpha4\beta3\delta$ receptors is a consequence of its ability to increase the duration of longer channel openings and their frequency, resulting in longer burst durations. By contrast, for muscimol, moderate superagonist behaviour was caused by reduced desensitisation of the extrasynaptic-type receptors. The ability to specifically increase the efficacy of receptor activation, by selected exogenous agonists over that obtained with the natural transmitter, may prove to be of therapeutic benefit under circumstances when synaptic inhibition is compromised or dysfunctional.

(Received 2 October 2009; accepted after revision 16 February 2010; first published online 22 February 2010)
Corresponding author T. G. Smart: Department of Neuroscience, Physiology and Pharmacology, University College London, Gower Street, London WC1E 6BT, UK. Email: t.smart@ucl.ac.uk

Abbreviations: *D*, desensitisation constant; *E*, efficacy; EC_{50}, effective concentration causing a 50% of maximum response; eGFP, enhanced green fluorescent protein; GABA, γ-aminobutyric acid; I_{max}, maximum current induced by GABA; M, transmembrane domain; P_O, open probability; THIP, 4,5,6,7-tetrahydoisoxazolo[5,4-c]pyridin-3(2*H*)-one; τ, time constant.

Introduction

Synaptic and extrasynaptic $GABA_A$ receptors play important roles in controlling neuronal excitability under physiological and pathophysiological conditions. These receptors are considered to be pentamers assembled from at least two α and two β subunits that additionally include either a single $\gamma2$ or δ subunit (Luscher & Keller, 2004). Although expression patterns for individual $GABA_A$ receptor subunits vary across the central nervous system, $\gamma2$ subunit-containing receptors are predominantly located at synaptic and extrasynaptic sites, whilst δ subunit receptors are thought to populate only extrasynaptic sites (Fritschy & Brunig, 2003). Together with other less common populations of $GABA_A$ receptors (Sieghart & Sperk, 2002), the different subunit compositions of $GABA_A$ receptors shape their biophysical and pharmacological properties and influence the efficacies of synaptic and tonic inhibition.

From neuronal and heterologous expression studies, it is clear that synaptic-type $GABA_A$ receptors share several features that include the ability to rapidly respond to a brief GABA concentration transient followed by a prolonged phase of deactivation. By contrast, extrasynaptic-type receptors are usually exposed to low but persistent GABA concentrations. They are also noted for their increased sensitivity to GABA, a reduced propensity to desensitise, and a more rapid deactivation phase following removal of

DOI: 10.1113/jphysiol.2009.182444

GABA compared to their synaptic counterparts (Gingrich *et al.* 1995; Banks & Pearce, 2000; Fischer *et al.* 2000; Yeung *et al.* 2003; Picton & Fisher, 2007; Lagrange *et al.* 2007).

Although synaptic and extrasynaptic receptors are differentially sensitive to some allosteric modulators (e.g. benzodiazepines and Zn^{2+}) their activation properties remain less well understood, particularly when exposed to different receptor agonists (Mortensen *et al.* 2004). Some agonists have unique activation profiles and certainly their chemical structures will affect the binding affinity and efficacy when initiating $GABA_A$ receptor activation. Of course, the receptor subunit composition will also affect ligand affinity and efficacy.

GABA is often considered a potent full agonist at $GABA_A$ receptors, but there are extrasynaptic isoforms, particularly associated with δ subunit-containing receptors, e.g. $\alpha4\beta3\delta$ (Adkins *et al.* 2001; Brown *et al.* 2002; You & Dunn, 2007), where it is a partial agonist by comparison with the high-efficacy behaviour of 4,5,6,7-tetrahydoisoxazolo[5,4-c]pyridin-3(2*H*)-one (THIP) (Krogsgaard-Larsen *et al.* 1994; Krogsgaard-Larsen *et al.* 2002). Interestingly, this high efficacy profile for THIP contrasts with its partial agonist activity on most other $\alpha\beta\gamma$-type $GABA_A$ receptors (Ebert *et al.* 1994; Mortensen *et al.* 2004).

The fundamental reasons why synaptic-type receptors such as $\alpha1\beta3\gamma2$ differ in their activation profile compared to extrasynaptic receptors such as $\alpha4\beta3\delta$, is poorly understood. In the present study, we have used GABA and two structurally related but conformationally constrained agonists, muscimol and THIP, to investigate the activation profiles of both synaptic and extrasynaptic receptors as well as that of the $\alpha4\beta3\gamma2$ receptor, which represents a convenient intermediary. We selected $\alpha1$ and $\alpha4$ subunit-containing receptors as these are widely expressed in the hippocampus and thalamus (Wisden *et al.* 1992; Sur *et al.* 1999; Sieghart & Sperk, 2002), which are areas where synaptic and tonic inhibition could profoundly affect behaviour.

Methods

Stable cell lines

Mouse L-tk fibroblast cell lines providing stable expression of human $\alpha1\beta3\gamma2$, $\alpha4\beta3\gamma2$ and $\alpha4\beta3\delta$ $GABA_A$ receptors were used. Expression of α, β and γ subunits was controlled by a dexamethasone inducible promoter (Hadingham *et al.* 1992; Sur *et al.* 1999; Brown *et al.* 2002), whilst δ subunits were expressed constitutively from a human CMV promoter (pcDNA3.1Zeo).

The L-tk cells were maintained in Dulbecco's modified Eagle's medium (DMEM) supplemented with: 4.5 mg ml^{-1} glucose, 4 mM L-glutamine, 0.11 mg ml^{-1} sodium pyruvate, 10% fetal calf serum (FCS), and 1 mg ml^{-1} geneticin at 37°C in 95% air–5% CO_2. The growth medium for $\alpha4\beta3\delta$ expressing cells also contained 0.2 mg ml^{-1} of zeocin for cell selection. Prior to electrophysiology, cells were washed once in Hanks' buffered salt solution, suspended with 2 ml 0.05% trypsin-EDTA, quenched with 10 ml medium, centrifuged for 3 min at 1000 *g*, triturated in 1 ml fresh medium with a polished glass pipette, and finally seeded at a suitable density onto poly D-lysine coated glass coverslips. The expression of the $GABA_A$ receptors was induced overnight in supplemented DMEM plus either 0.1 μM dexamethasone for $\alpha1\beta3\gamma2$ and $\alpha4\beta3\gamma2$ or 0.5 μM dexamethasone for $\alpha4\beta3\delta$. Electrophysiological recordings were performed within 48 h of inducing receptor expression.

Transient receptor expression in HEK cells

Human embryonic kidney 293 (HEK293) cells were maintained in DMEM supplemented with: 4.5 mg ml^{-1} glucose, 4 mM L-glutamine, 0.11 mg ml^{-1} sodium pyruvate, 10% FCS, 100 units ml^{-1} penicillin-G and 100 μg ml^{-1} streptomycin at 37°C in 95% air–5% CO_2. Cells at ∼70% confluence were passaged at 1:10 usually every 2–4 days. Cells were plated onto poly D-lysine coated glass coverslips, and subsequently transfected using a calcium phosphate method for cDNAs encoding murine $\alpha1$, $\alpha4$, $\beta3$, $\gamma2$ and δ subunits and the reporter enhanced green fluorescent protein (eGFP). For a$1\beta3\gamma2$/eGFP and $\alpha4\beta3\gamma2$/eGFP each dish was transfected with 4 μg of cDNA in a 1:1:1:1 ratio, whereas 7 μg of cDNA was used for $\alpha4\beta3\delta$/eGFP in a ratio of 1:1:4:1. Cells were incubated overnight and used for patch clamp recording the following day.

Electrophysiology

Agonist-activated whole-cell and single channel currents were recorded with an Axopatch 200B amplifier (Molecular Devices, Sunnyvale, CA, USA). Cells were voltage clamped at −60 mV, whereas for single channels, outside-out patches were held at a holding potential of −70 mV. Whole-cell currents were filtered at 5 kHz and single channel currents at 3 kHz (−3 dB, 8 pole Bessel, 48 dB/octave). For whole-cell currents, the series resistance was 20 ± 10 MΩ and compensation was routinely applied up to approximately 75%. All currents were digitized at 50 kHz via a Digidata 1320A (Molecular Devices) and recorded straight to disk (Dell Pentium Dual Core – Optiplex GX745). Patch pipettes with a resistance of 3–5 MΩ for whole-cell and 10–15 MΩ for single channels were filled with an intracellular solution containing (mM): 120 CsCl, 1 $MgCl_2$, 11 EGTA, 33 TEA-OH, 10 Hepes, 1 $CaCl_2$ and 2 adenosine triphosphate; pH 7.10 (adjusted

with 1 M HCl). Cells were continuously perfused with Krebs solution containing (mM): 140 NaCl, 4.7 KCl, 1.2 $MgCl_2$, 2.52 $CaCl_2$, 11 glucose and 5 Hepes; pH 7.4 (adjusted with 1 M NaOH).

Agonists were applied to cells using a U-tube application system (Mortensen & Smart, 2007). Drugs were dissolved in the extracellular Krebs solution followed by pH correction. Only THIP changed the pH of the Krebs solution at the highest concentrations (10 mM; unadjusted $\sim$ pH 4.0). For those experiments that addressed the issue of pH on the single channel conductance, 10 mM GABA was also adjusted to pH 4.0 (with 1 M HCl).

Analysis of whole-cell currents

GABA, muscimol and THIP equilibrium concentration–response relationships were constructed for each receptor isoform by measuring agonist currents, which were normalized to the response induced by a maximal, saturating concentration of GABA (I_{max}) and subsequently fitted with the Hill equation:

$$I/I_{max} = [1/(1 + (EC_{50}/[A])^n)], \quad (1)$$

where EC_{50} represents the concentration of the agonist ([A]) inducing 50% of the maximal current evoked by a saturating concentration of the agonist and n represents the Hill coefficient.

In order to obtain preliminary estimates of affinity, efficacy and desensitization, whole-cell concentration–response curves were also fitted to a function based on the receptor mechanism (Mortensen *et al.* 2004) shown in Scheme 1.

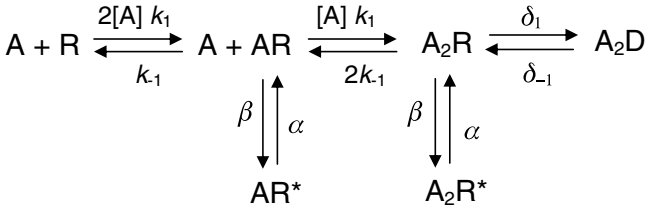

where A represents an agonist molecule and R the $GABA_A$ receptor, with rate constants for binding (k_1) and unbinding (k_{-1}), and rate constants for channel opening (β) and closure (α). To reduce the number of variables in the fitting process, the binding rate constants were constrained to be identical for mono- and biliganded binding. This condition also applied to the unbinding rates. The channel gating rates (β, α) for mono- and biliganded receptors were also similarly constrained. The activated conducting forms of the receptor are represented by AR* and A_2R^*. A desensitised state of the receptor (D) has entry and exit rate constants denoted by δ_1 and δ_{-1}, respectively. The AR* state was considered rare and discounted from the fitting. Under these conditions, the general function derived for this mechanism, is:

$$P_{open} = ([A]^n E/(([A] + K)^n + [A]^n(E + D))), \quad (2)$$

where n signifies the number of ligand binding sites. As $[A] \to \infty$, $P_{open} \to P_{open,max}$, which is given by $E/(1 + E + D)$. The dissociation constant (K) is defined as k_{-1}/k_1; efficacy (E) is defined as β/α; and D is defined as δ_1/δ_{-1}. A non-linear least squares routine was used to fit the concentration–response curves (Mortensen *et al.* 2004).

Single channel current analysis

Single channel currents were recorded at -70 mV on the condition that there appeared to be only one active channel, or the number of simultaneous channel openings never exceeded 2% of all detected openings. SCAN, EKDIST (http://www.ucl.ac.uk/Pharmacology/dcpr95.html) and QuB (http://www.qub.buffalo.edu) software were used to analyse the single channel currents. The single channel current amplitude histograms were fitted with the sum of Gaussian components to define the single channel conductance states as described previously (Mortensen *et al.* 2004). Dwell time frequency distributions were constructed from the channel open and closed durations and analysed by fitting mixtures of exponential densities using the EKDIST program after imposing a minimum time resolution of 100 μs. The burst length analyses required a critical shut time (τ_{crit}; usually between τ_{C2} (denoting closures within a burst) and τ_{C3} (closures outside bursts)), which was defined as described previously (Colquhoun & Sakmann, 1985; Mortensen *et al.* 2004; Mortensen & Smart, 2007).

Kinetic modelling of single channel currents

An extensive search for an optimal receptor model that could account for our experimental single channel data resulted in 30 different models being analysed using the HJCFIT program (Hatton *et al.* 2003) for GABA-activated channels on $\alpha1\beta2\gamma2$ receptors (data not shown). Some of these models included extra desensitised states branching from the mono- and biliganded receptor states, as well as the inclusion of preactivation flip states which are closed agonist-bound states prior to channel activation (Supplemental Fig. 1*F* and *G*) and are capable of accounting for some GABA receptor single channel kinetic behaviour (Keramidas & Harrison, 2009). Despite these increasing levels of branching complexity, we found that none of the above models achieved a better description of the single channel data than our previously published six-state model (2 open, 4 closed; see above). Therefore,

this model was adopted for the present study (Mortensen *et al.* 2004).

Clusters of channel openings for each isoform of the $GABA_A$ receptor, $\alpha1\beta3\gamma2$, $\alpha4\beta3\gamma2$ or $\alpha4\beta3\delta$, were idealised using the segmental-k-means method (SKM) in QuB (Qin *et al.* 1996; Qin, 2004). Multiple files of idealised single channel data from each of the three concentrations of the same agonist were used in QuB to determine the rate constants for the model that could describe the dwell time distributions. Using maximum interval likelihood rate estimation (MIL), which includes a correction for missed events, the determined optimal rate constants for transitions between states were robust, even when quite different starting estimates were used. We also used maximum likelihood fitting of our receptor mechanism to the single channel data, which included an exact correction for missed events, with the program HJCFIT (Hatton *et al.* 2003). For the single channel experiments, the binding and unbinding rate constants (k_1, k_{-1}, k_2 and k_{-2}), and the opening and shutting rate constants (β_1, β_2, α_1 and α_2) were no longer constrained in the receptor model (see below). The dwell time distributions and the fit of multiple exponential densities were exported to Origin v. 6 (OriginLab Corp., Northampton, MA, USA) to create the 3D dwell-time distributions (Scheme 2).

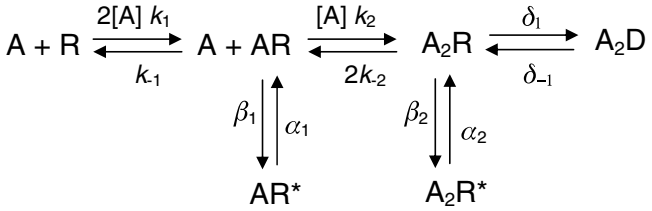

Simulated whole-cell concentration response curves

The optimal single channel rate constants determined from fitting the single channel data with the receptor model using QuB were transferred to ChanneLab v. 2 (Synaptosoft, Decatur, GA, USA), where the linear/branched receptor model was recreated. Whole-cell responses were simulated by using a number of channels, set at 1000, a holding current of −60 mV, and 4 s agonist applications, to reproduce our original whole-cell experiments. The peak of the simulated whole-cell currents was measured (pA) for different agonist concentrations. These values were used to generate the theoretical agonist concentration–response curves using Origin 6.

Results

To understand the biophysical behaviour of different GABA agonists at synaptic and extrasynaptic $GABA_A$ receptors, we chose to compare the activity of GABA with muscimol and THIP. GABA was selected since it is the natural transmitter and would act as a 'control'; muscimol was selected because of its greater potency at most $GABA_A$ receptors; and THIP was selected due to its superagonist activity at δ subunit-containing receptors, which are associated with extrasynaptic $GABA_A$ receptors. Although the structures of these three agonists appear quite similar, they display different degrees of conformational flexibility from the highly flexible GABA, to the constrained isoxazole ring structures of muscimol and also THIP, which is further constrained by a pyridine ring (Fig. 1*A*) (Krogsgaard-Larsen *et al.* 1977).

Agonist potencies and relative efficacies from whole-cell currents

We investigated the activity of the three agonists at synaptic- and extrasynaptic-type, $\alpha1\beta3\gamma2$, $\alpha4\beta3\gamma2$ and $\alpha4\beta3\delta$ receptors, expressed in L-tk cells. Agonist concentration–response curves were constructed for GABA-, muscimol- and THIP-activated currents recorded under whole-cell voltage clamp conditions (V_H −60 mV; Fig. 1*B*). The agonist-induced maximum currents were larger for $\alpha1\beta3\gamma2$ and $\alpha4\beta3\gamma2$ receptors than for $\alpha4\beta3\delta$ $GABA_A$ receptors ($\alpha1\beta3\gamma2$, $I_{max,GABA}$: 1742 ± 303 pA; $\alpha4\beta3\gamma2$, $I_{max,GABA}$: 1767 ± 253 pA; $\alpha4\beta3\delta$, $I_{max,THIP}$: 851 ± 128 pA, $n = 5$–7; $P < 0.05$). Receptor desensitization was observed with high agonist concentrations, which was most evident for $\gamma2$ subunit-containing receptors, but also noticeable for the $\alpha4\beta3\delta$ isoform (Fig. 1*C*).

For both the $\alpha1\beta3\gamma2$ and $\alpha4\beta3\gamma2$ receptors, muscimol behaved as a full agonist, like GABA, with comparable maximal currents at saturating concentrations (101 ± 1.7% and 97 ± 3.7% of $I_{max,GABA,}$ respectively). However, by comparing EC_{50} values, muscimol was more potent by approximately 3-fold ($\alpha1\beta3\gamma2$: muscimol $EC_{50} = 0.92 \pm 0.65$ μM, GABA 3.4 ± 0.75 μM; $P = 0.037$; $\alpha4\beta3\gamma2$: muscimol 0.69 ± 0.25 μM, GABA 2.1 ± 0.46 μM; $P = 0.032$, $n = 5$–7, Fig. 1*B*; Table 1). By contrast, THIP behaved as a partial agonist on both $\alpha1\beta3\gamma2$ and $\alpha4\beta3\gamma2$ receptors (85 ± 2.7% and 83 ± 4.7% of $I_{max,GABA}$, respectively), and was also significantly less potent than either GABA or muscimol ($\alpha1\beta3\gamma2$: $EC_{50} = 107 \pm 31$ μM, $P = 0.002$; $\alpha4\beta3\gamma2$: 69 ± 1.2 μM, $P = 0.0001$; ANOVA, $n = 6$).

For $\alpha4\beta3\delta$ $GABA_A$ receptors, the increased maximum response to muscimol compared to GABA (120 ± 5.1%; $P = 0.006$, $n = 6$) implied a degree of superagonist activity. For THIP, this type of behaviour was clearly evident (224 ± 9.3% of $I_{max,GABA}$, $P = 0.0001$, $n = 6$). In comparison with the synaptic-type $\alpha1\beta3\gamma2$ receptors,

Table 1. Whole-cell current parameters for GABA, muscimol and THIP on $\alpha1\beta3\gamma2$, $\alpha4\beta3\gamma2$ and $\alpha4\beta3\delta$ $GABA_A$ receptors

Isoform	Agonist	E_{max} (%)	EC_{50} (μM)	n_H	$EC_{low,mid,high}$ (μM)
$\alpha1\beta3\gamma2$	GABA	100 ± 0.7	3.4 ± 1.0	1.4 ± 0.16	0.3, 3, 30
	Muscimol	101 ± 1.7	0.92 ± 0.34	1.2 ± 0.17	0.03, 0.3, 3
	THIP	85 ± 2.7	107 ± 31	1.2 ± 0.07	3, 30, 300
$\alpha4\beta3\gamma2$	GABA	98 ± 0.65	2.1 ± 0.56	1.5 ± 0.16	0.3, 3, 30
	Muscimol	97 ± 3.7	0.69 ± 0.25	1.46 ± 0.22	0.03, 0.3, 3
	THIP	83 ± 4.7	69 ± 1.2	1.3 ± 0.08	3, 30, 300
$\alpha4\beta3\delta$	GABA	98 ± 0.67	0.35 ± 0.03	1.1 ± 0.05	0.03, 0.3, 3
	Muscimol	120 ± 5.1	0.20 ± 0.04	0.97 ± 0.15	0.03, 0.3, 3
	THIP	224 ± 9.3	13 ± 3.5	0.88 ± 0.05	3, 30, 300

The data were obtained from 5–7 experiments on L-tk cells stably expressing $\alpha1\beta3\gamma2$, $\alpha4\beta3\gamma2$ or $\alpha4\beta3\delta$ $GABA_A$ receptors. The Hill equation was fitted to each individual data set and the mean parameter values are shown in the table as means $\pm$ S.E.M. E_{max} is the % maximum agonist-induced current. EC_{50} represents the agonist potency and n_H, the Hill slope. The agonist concentrations selected for the single channel experiments were in the range of EC of ~15 (EC_{low}), ~50 (EC_{mid}), and ~90 (EC_{high}).

GABA, muscimol and THIP were more potent in activating the $\alpha4\beta3\delta$ receptor ($EC_{50} = 0.35 \pm 0.03$ μM ($P = 0.002$), 0.20 ± 0.04 μM ($P = 0.03$) and 13 ± 3.5 μM ($P = 0.01$), respectively, $n = 6$–7; Table 1).

Next, all of the agonist concentration–response relationships were curve fitted using our linear/branched receptor model (see Methods; Mortensen *et al.* 2004) to obtain estimates of the agonist dissociation constant (K),

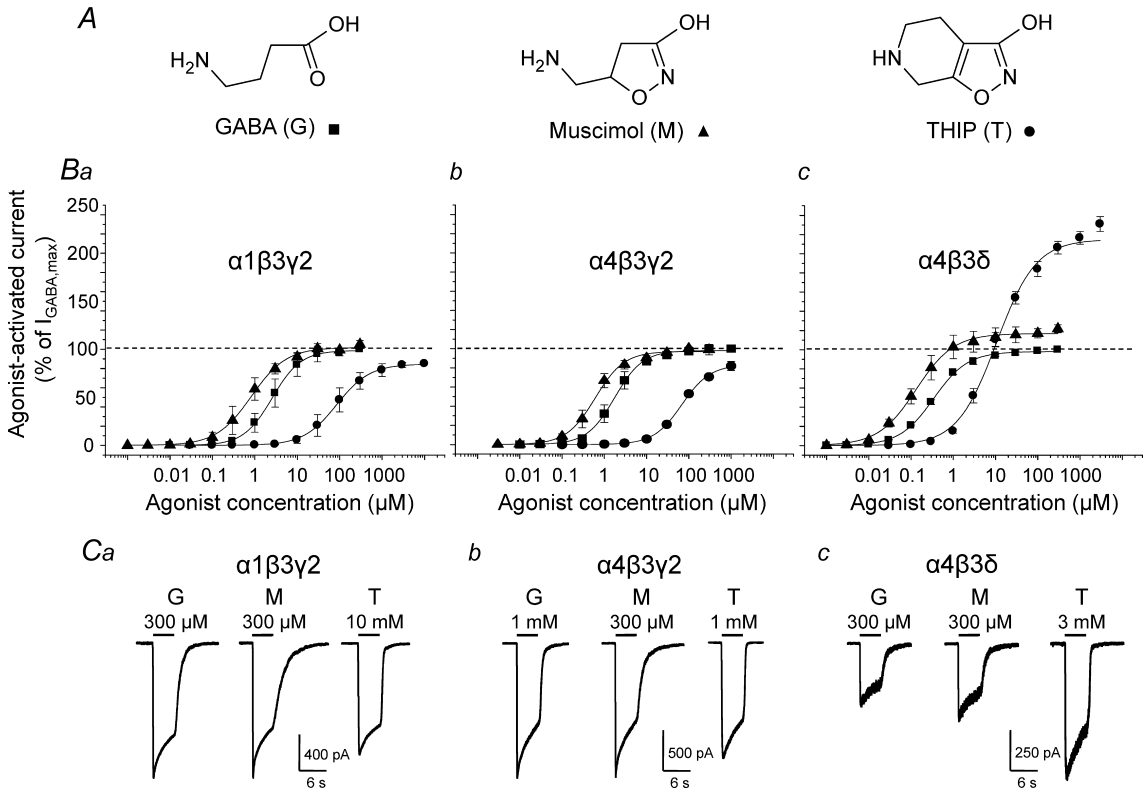

Figure 1. Activation of recombinant synaptic and extrasynaptic $GABA_A$ receptors by three agonists
A, structures of the selective $GABA_A$ receptor agonists: GABA (square), muscimol (triangle) and THIP (circle). The agonists are labelled G (GABA), M (muscimol) and T (THIP) in this and subsequent figures. *B*, agonist concentration–response relationships for GABA, muscimol and THIP on recombinant $\alpha1\beta3\gamma2$ (*a*), $\alpha4\beta3\gamma2$ (*b*) and $\alpha4\beta3\delta$ (*c*) receptors expressed in L-tk cells ($n = 5$–7; mean $\pm$ S.E.M.). *C*, whole cell currents induced by saturating concentrations of GABA, muscimol and THIP on recombinant $\alpha1\beta3\gamma2$ (*a*), $\alpha4\beta3\gamma2$ (*b*) and $\alpha4\beta3\delta$ (*c*).

Table 2. Efficacies, dissociation and desensitization constants and slope factors obtained for GABA, muscimol and THIP on $\alpha1\beta3\gamma2$, $\alpha4\beta3\gamma2$ and $\alpha4\beta3\delta$ $GABA_A$ receptors

Isoform	Agonist	*E*	*D*	*K* (μM)	*n*
$\alpha1\beta3\gamma2$	GABA	8.3 ± 0.12	5.6 ± 0.07	16 ± 2	1.38 ± 0.06
	Muscimol	8.8 ± 0.24	5.6 ± 0.14	10 ± 2	1.08 ± 0.08
	THIP	3.2 ± 0.32	2.6 ± 0.38	400 ± 8	1.18 ± 0.04
$\alpha4\beta3\gamma2$	GABA	3.3 ± 0.05	1.7 ± 0.04	3.9 ± 0.6	1.60 ± 0.09
	Muscimol	2.7 ± 0.07	1.2 ± 0.05	1.2 ± 0.3	1.57 ± 0.20
	THIP	3.2 ± 0.08	2.5 ± 0.09	250 ± 40	1.37 ± 0.09
$\alpha4\beta3\delta$	GABA	1.8 ± 0.03	0.50 ± 0.02	0.84 ± 0.11	1.17 ± 0.07
	Muscimol	1.9 ± 0.04	0.50 ± 0.03	0.44 ± 0.09	1.00 ± 0.09
	THIP	6.0 ± 0.24	4.0 ± 0.19	121 ± 14	0.99 ± 0.03

The agonist concentration–response data in Fig. 1*B* was fitted using our linear/branched receptor model (eqn (2) in Methods; Mortensen *et al.* 2004). A non-linear least squares fitting routine was used to obtain the estimates of *E* (efficacy), *K* (dissociation constant), *D* (desensitisation constant) and *n* (slope factor). Values are means $\pm$ S.E.M. from 5–7 experiments.

its efficacy (E), and desensitisation (D), without discerning between monoliganded and biliganded receptor states so as to reduce the number of variables in the fitting routine (Table 2). These fits predicted that K is higher for THIP compared to GABA and muscimol at all three receptors; that the efficacy of THIP, which is low at γ subunit-containing receptors, is highest at the $\alpha4\beta3\delta$ receptors; and finally, the extent of desensitisation of $\alpha4\beta3\delta$ receptors is greater with THIP compared to either GABA or muscimol. Of course, we cannot guarantee accurate values for K, D and E by just fitting agonist concentration response relationships. In addition, it should be noted that the state function (eqn (2)) used to fit the concentration–response curve data, is most appropriate for receptors at equilibrium and this may not be the case for peak currents evoked by each of the three agonists, particularly at the $\alpha1\beta3\gamma2$ receptor using a U-tube with a solution exchange time of 27 ± 6 ms ($n = 5$). Thus the determinants of K, D and E from dose–response curve data are only to be considered as estimates.

Therefore, to investigate further, we used the agonist concentration response curves to select three concentrations for each agonist, defined as low, mid and high (EC_{low} ($\sim$15% of max), EC_{mid} ($\sim$50%), EC_{high} ($\sim$90%)), for single channel experiments (Table 1). This range enabled the kinetics of single GABA channels to be investigated at concentrations that resulted in super-agonist activity as well as submaximal responses, enabling more precise determinations of K, D and E.

Single GABA channel conductances are unaffected by the agonist

Outside-out patches were pulled from L-tk cells and single channel activity induced by GABA, muscimol and THIP at -70 mV was recorded at three concentrations under equilibrium conditions from each receptor isoform. The recordings revealed no differences in the single channel current amplitudes between the agonists (Fig. 2*A*–*C*). Three different conductance levels were usually identified from amplitude histograms constructed for currents activated by GABA, THIP and muscimol. For all three receptor isoforms, the channel conductances equated to: 11–14 pS, 17–21 pS, and 26–31 pS (Fig. 2*D* and *E*). These conductance states did not vary with the receptor isoform, the activating agonist, or its concentration (Fig. 2*E*). By examining the frequencies for all the channel conductances, it was clear that openings to the highest conductance state dominated all the recordings (60–90%; Fig. 2*F*).

Low pH can modulate agonist-activated channels

The superagonist behaviour of THIP at only $\alpha\beta\delta$ extrasynaptic-type receptors makes this a useful ligand for distinguishing δ from $\gamma2$ subunit-containing receptors. By using $\beta2$ subunit-containing receptors, part of THIP's superagonist effect was thought to be due to an increase in the single channel conductance from 25 to 36 pS at both $\alpha1\beta2\gamma2$ and $\alpha1\beta2\delta$ receptors (Keramidas & Harrison, 2008). Such an increase was not observed in our study of receptors containing $\beta3$ subunits. However, aqueous solutions of THIP (HCl salt) are very acidic, particularly at high concentrations (10 mM), which reduced the pH of the Krebs solution from 7.4 to $\sim$4.0 (Matsuda *et al.* 1996). During a previous study (Mortensen *et al.* 2004), using $\alpha1\beta2\gamma2$ receptors, we noted that if THIP was applied to outside-out patches without pH correction to the normal physiological range, changes to the channel conductance were apparent.

To reaffirm, we applied without pH correction a saturating concentration of THIP (10 mM) to HEK cell outside-out patches containing either $\alpha1\beta3\gamma2$ (Fig. 3*A–D*) or $\alpha4\beta3\delta$ (Fig. 3*E*) murine receptors. The maximum single channel current was increased from 27 ± 0.7 pS and 25 ± 0.4 pS at pH 7.4 ($n = 6$–7) to 37 ± 0.7 pS and 41 ± 1.9 pS at pH 4, respectively ($n = 6$–9; Fig. 3*D* and *E*). These increments to 137% ($\alpha1\beta3\gamma2$) and 164% ($\alpha4\beta3\delta$) in the most frequently occurring single channel current state, were not specific to THIP since GABA similarly increased channel current after lowering external pH from 7.4 to 4 (Fig. 3*D* and *E*). Moreover, whilst recording from the same patches expressing $\alpha1\beta3\gamma2$ or $\alpha4\beta3\delta$ receptors, readjusting the external pH from 4 to 7.4 or 7.4 to 4, caused the main conductance state activated by 10 mM THIP or 10 mM GABA to be either reduced or increased (Fig. 3*A–C*).

THIP modulates channel open probability and mean open times

Another parameter that will affect the function of synaptic and extrasynaptic-type receptors is the open probability (P_O). The number of channels in a patch will significantly affect P_O, and although we cannot be sure of channel numbers, the occurrence of 'channel current stacking' was quite infrequent. Nevertheless, to avoid this common problem, we measured P_O by only analysing clusters of channel activity. These cluster P_O values increased with the agonist concentration as would be expected.

Interestingly, $\alpha4$ subunit-containing receptors exhibited a smaller range for P_O compared with that for $\alpha1\beta3\gamma2$ receptors, indicating that $\alpha4\beta3\gamma2$ receptors are likely to be less efficient at charge transfer (Fig. 4). For $\alpha1\beta3\gamma2$ receptors activated by mid and high THIP concentrations,

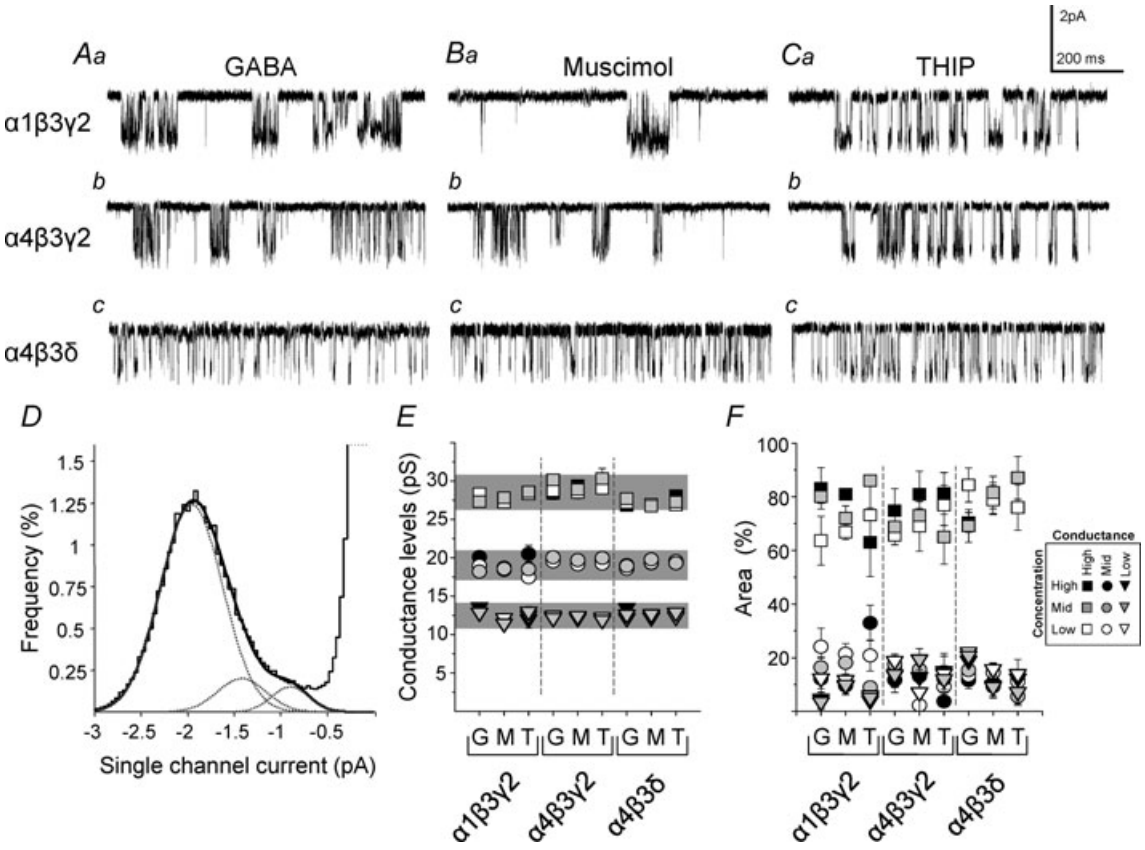

Figure 2. Single channels have three identical conductance levels for synaptic- and extrasynaptic-type $GABA_A$ receptors

A–C, single channel currents induced by GABA (*A*), muscimol (*B*) and THIP (*C*) on recombinant $\alpha1\beta3\gamma2$ (*a*), $\alpha4\beta3\gamma2$ (*b*) and $\alpha4\beta3\delta$ (*c*) receptors. *D*, typical current amplitude histogram ($\alpha1\beta3\gamma2$, 3 μM GABA) showing curve fits with three Gaussians each (dotted lines) and their sum (continuous line). *E*, three conductance levels (high, 26–31 pS (squares); intermediate, 17–22 pS (circles); low, 11–14 pS (triangles)) were resolved for all three agonists at three concentrations (low EC_{5-20} (white); intermediate EC_{40-60} (grey); and high EC_{80-100} (black)) ($n = 5$–7; mean ± S.E.M.). See Table 1 for agonist concentrations. *F*, relative areas of the single channel conductances for all three agonists at each receptor isoform, at three concentrations.

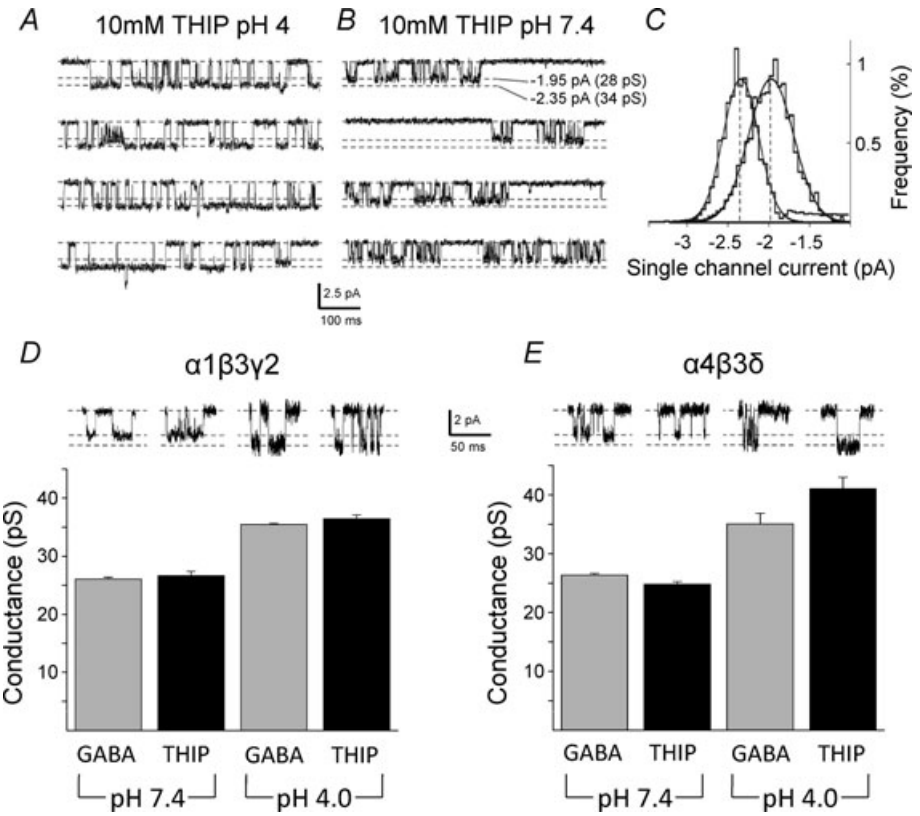

Figure 3. Low external pH affects the single channel conductance
A and *B*, single channel currents induced by high concentrations of THIP at recombinant synaptic-type $\alpha1\beta3\gamma2$ receptors exposed to pH 4 or 7.4 external solution. *C*, displacement of the single channel current amplitude histogram by pH 4 (left) from pH 7.4 (right). *D* and *E*, single channel main state conductances for synaptic-type $\alpha1\beta3\gamma2$ and extrasynaptic-type $\alpha4\beta3\delta$ $GABA_A$ receptors for both GABA (10 mM) and THIP (10 mM) at pH 4.0 and 7.4. Sample currents are shown in the insets.

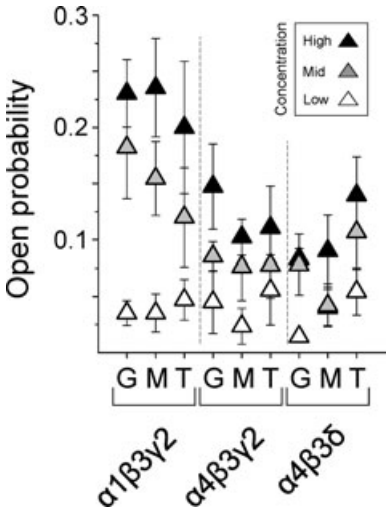

Figure 4. Channel open probability is affected by the receptor isoform and agonist concentration
Open probability was measured by analysing clusters of channel activity induced by the three concentrations (see Table 1) of GABA (G), muscimol (M) and THIP (T). Data are means ± S.E.M. $n = 5$–7.

there was a tendency towards lower P_O values compared with either GABA or muscimol. However, at the highest concentration of THIP, $\alpha4\beta3\delta$ receptors had a tendency towards a higher mean cluster P_O, which would contribute towards the superagonist activity of THIP at high concentrations (Fig. 4).

Next, we assessed the mean open times for channels activated by all three agonists at each receptor isoform. Overall, the mean open time increased with the agonist concentration. This was most pronounced for $\alpha1\beta3\gamma2$ receptors compared to $\alpha4$ subunit-containing receptors (Fig. 5*A*). Furthermore, the longest mean open times, at the highest agonist concentrations, were also consistently longer for $\alpha1\beta3\gamma2$ compared with $\alpha4\beta3\gamma2$ receptors. For the extrasynaptic-type $\alpha4\beta3\delta$ receptors, the highest concentration of the superagonist THIP resulted in significantly longer mean open times ($P < 0.05$) compared with either GABA or muscimol (Fig. 5*A*).

As the mean open time is a weighted value of discrete open time constants, we analysed the underlying individual open time distributions. These were optimally fitted by two exponentials (based on an *F* test and visual

evaluation of the fits), indicating that two populations of open time durations were present for all three receptors activated by all concentrations of the different agonists (Fig. 5*Ba–c*). The open time constant (τ_{O1}) describing the shortest open times was invariant at 0.2–0.4 ms, irrespective of the receptor isoform, the type of agonist, or its concentration. By contrast, the longer open time constant (τ_{O2}) was variable being longest for channel openings of $\alpha1\beta3\gamma2$ receptors compared to the shorter values for $\alpha4\beta3\gamma2$ receptors (Fig. 5*Ca*). With regard to the extrasynaptic-type $\alpha4\beta3\delta$ receptors and the super-agonist activity of THIP, it was notable that at the highest concentrations, THIP resulted in a significantly greater τ_{O2} compared with that for either GABA or muscimol ($P < 0.05$; Fig. 5*Ca* and *D*).

By considering the relative frequencies of channel openings, events that can be assigned to the short open time population dominated (70–80%) over those of the longer open time population (20–30%) at low concentrations of all three agonists on $\alpha1\beta3\gamma2$ receptors (Fig. 5*Cb*). However, at higher agonist concentrations, the frequencies of the two populations were similar. For the $\alpha4$ subunit-containing receptors, the relative frequencies exhibited a narrower range. The long open time population tended to dominate (~65%) at the highest concentrations of GABA and THIP on $\alpha4\beta3\delta$ receptors (Fig. 5*Cb*).

Channel burst activity differs at $\alpha1$ and $\alpha4$ subunit-containing receptors

The closed times between openings are generally complex with the briefest closures appearing within bursts, and longer closures reflecting either sojourns of the receptor in unbound states (usually in the presence of lower agonist concentrations) or in desensitized states (common with higher agonist concentrations). By analysing the

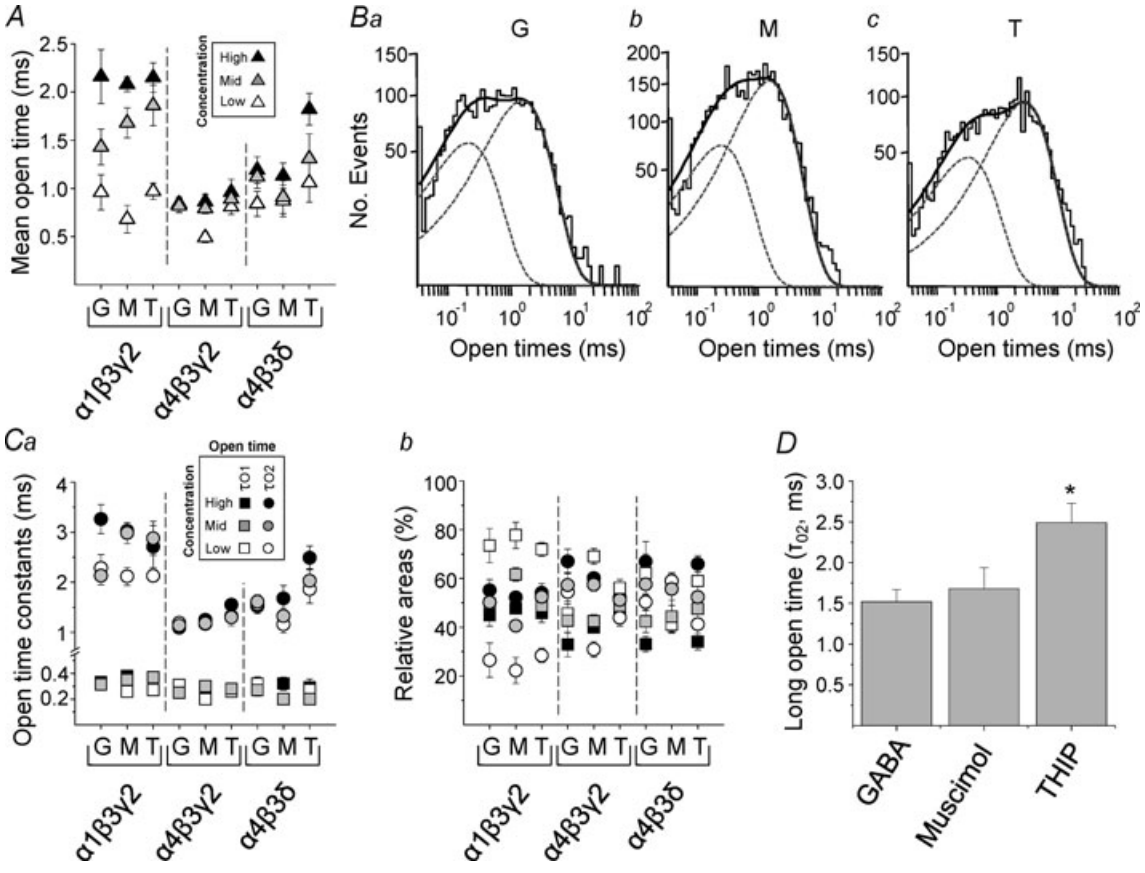

Figure 5. Open times vary with the receptor isoform and agonist concentration
A, mean open times for GABA (G), muscimol (M) and THIP (T) at three concentrations for $\alpha1\beta3\gamma2$, $\alpha4\beta3\gamma2$ or $\alpha4\beta3\delta$ receptors. *B*, open time distributions for GABA (3 μM; *a*), muscimol (3 μM; *b*) and THIP (300 μM; c) on $\alpha4\beta3\delta$ receptors, each showing two exponentials (dotted lines) and their sum (continuous line). *C*, open time constants (*a*; short τ_{O1}, squares; and long τ_{O2}, circles) and their relative areas (*b*) determined from exponential fits to the open time constant distributions. *D*, bar graph of the long open times (τ_{O2}) for THIP compared with GABA and muscimol on $\alpha4\beta3\delta$ receptors (*$P = 0.0136$; ANOVA, $n = 6–7$).

distribution of all closed states for each receptor, four populations of closed times were resolved at lower agonist concentrations, increasing to five at higher agonist concentrations, especially if very long desensitised periods were resolved (as for $\alpha1\beta3\gamma2$ receptors; data not shown).

The two shortest closed time constants (τ_{C1} and τ_{C2}) were unaffected by the agonist concentration, which is an indication that such closures most likely occur within bursts of channel activity (intraburst closures; Fig. 6*A*). The mean values for τ_{C1} were noticeably greater for $\alpha4\beta3\gamma2$ receptors, whereas τ_{C2} was fractionally greater on $\alpha4\beta3\delta$ receptors when compared with closed time constants for the other receptor isoforms (Fig. 6*A*). The longer closed times between bursts were not considered further as they are confounded by the uncertainty over the number of active channels present in the patch.

By examining the closed time frequencies for the brief intraburst closures with high concentrations of GABA and muscimol on $\alpha1\beta3\gamma2$ receptors, the most frequent closures (~70%) were defined by the population described by τ_{C1} (Fig. 6*B*). This reflected the apparent propensity of $\alpha1\beta3\gamma2$ receptors to enter into long bursts of briefly spaced openings induced by the high efficacy agonists. The frequency of short closures was far less evident for the extrasynaptic-type $\alpha4\beta3\delta$ receptors. This partly explained their shorter burst behaviour (Fig. 6*B*).

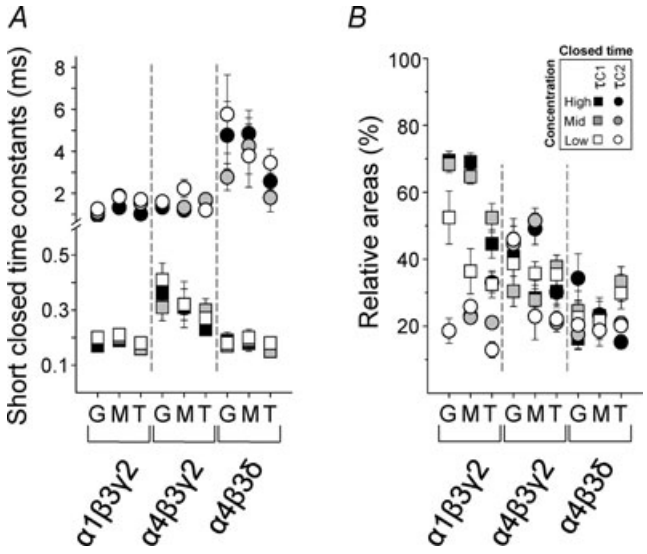

Figure 6. Intraburst closed time relationships for synaptic- and extrasynaptic-type $GABA_A$ receptors
A, closed time constants determined from distributions of short closed times (τ_{C1} (squares) and τ_{C2} (circles)) representing closed times within bursts of channel activity induced by GABA (G), muscimol (M) and THIP (T) at low, mid and high concentrations. *B*, relative areas for the intraburst closed times, τ_{C1} and τ_{C2}. $n = 5$–7 experiments.

THIP critically increases burst durations of $\alpha4\beta3\delta$ receptors

The steady-state activation of each receptor by GABA, muscimol and THIP produced clusters of channel openings with distinct features (Fig. 2*A*–*C*; 7*A*). For $\alpha1\beta3\gamma2$ receptors, agonist activation produced long clusters of openings characterised by successive discrete bursts of channel activity (Fig. 7*Aa*). Such lengthy clusters were rarely observed following activation of either $\alpha4\beta3\gamma2$ or $\alpha4\beta3\delta$ receptors by GABA, muscimol or THIP (Fig. 2*A*–*C*; 7*Ab* and *c*) preventing a satisfactory cluster analysis. We therefore analysed burst durations having first defined bursts of activity using a critical closed time (τ_{crit}) determined between τ_{C2} and τ_{C3}. As closed times shorter than τ_{crit} (τ_{C1} and τ_{C2}) were unaffected by agonist concentration, these were assumed to represent intraburst closures, whereas the agonist concentration-dependent closed times longer than τ_{crit} (τ_{C3} to τ_{C5}) probably reflected closures between bursts.

Analysis of mean burst durations showed that these increased with the concentration of the agonists as would be expected. Higher concentrations of GABA and especially muscimol resulted in longer bursts compared to those induced by THIP on $\alpha1\beta3\gamma2$ receptors (Fig. 7*C*). However, mean burst durations for $\alpha4$ subunit-containing receptors exhibited a much narrower range and were generally shorter than for $\alpha1\beta3\gamma2$ receptors (Fig. 7*C*). For the $\alpha4\beta3\gamma2$ receptors, GABA induced longer bursts compared to the other agonists, whilst for $\alpha4\beta3\delta$ receptors, the highest concentration of THIP induced significantly longer bursts compared to either GABA or muscimol ($P < 0.05$; $n = 7$–8; Fig. 7*C* and *D*).

Fitting the distributions of all burst durations with exponential functions suggested that two or three populations of burst durations accounted for the activity of $\alpha1\beta3\gamma2$ receptors. By contrast, two exponential densities were adequate for $\alpha4\beta3\gamma2$ and $\alpha4\beta3\delta$ receptors (Fig. 7*Ba*–*c*). The mean number of openings per burst for $\alpha1\beta3\gamma2$ receptors was increased with higher concentrations of GABA and muscimol compared with $\alpha4\beta3\gamma2$ or $\alpha4\beta3\delta$ receptors (Fig. 7*E*). Interestingly, the mean number of openings per burst for $\alpha4\beta3\delta$ receptors was particularly low (~2) for all agonists, which explains the brevity of the bursts (Fig. 7*Ac*). Taken overall, THIP therefore prolongs the burst duration of $\alpha4\beta3\delta$ receptors, compared to GABA and muscimol, without increasing the number of openings per burst.

Modelling synaptic- and extrasynaptic-type $GABA_A$ receptor behaviour

To evaluate the differences between the binding to and gating of $\alpha1\beta3\gamma2$, $\alpha4\beta3\gamma2$ and $\alpha4\beta3\delta$ receptors by the

agonists, we devised a number of kinetic models to account for their single channel behaviour. We investigated many different models concentrating mainly on those with two open states and at least three closed states. Overall, this extended analysis (data not shown) indicated that none of the more complex models provided fits to our data that were clearly superior to those provided by the linear-branched model used previously (Mortensen *et al.* 2004). This model allowed two agonist molecules to bind to the receptor with monoliganded and biliganded channel openings to a main state conductance. A desensitised state accessed from the bilganded state was also incorporated (Fig. 8*A*). We used this model, and initial values for the rate and conformation constants, based on our previous study, to begin accounting for the single channel behaviour of $\alpha1\beta3\gamma2$ receptors, following activation by each agonist at each concentration. The final iterated rate constants were then used to generate fits to the open and closed time distributions for each agonist at all three concentrations (Supplemental Fig. 2*Aa–Cb*).

For GABA and muscimol, the model predicts little change in the gating of the $\alpha1\beta3\gamma2$ channel, or its entry into and exit from desensitisation. The greater potency of muscimol, evident from the concentration–response curves, must therefore depend upon the faster forward rate constants for agonist binding (Table 3; Supplemental Fig. 2*Ac, Bc*). For THIP activation of $\alpha1\beta3\gamma2$ receptors, the rates of channel opening ($\beta1$ and $\beta2$), are considerably slower compared with those for GABA and muscimol and the binding rate constants (k_1, k_2) are also reduced (Table 3; Supplemental Fig. 2*Cc*) resulting in the displaced concentration–response curve for THIP towards higher agonist concentrations and the slightly reduced maximum response (Fig. 1*Ba*).

By exchanging the $\alpha1$ subunit for $\alpha4$, the forward and backward rate constants for agonist binding/unbinding at $\alpha4\beta3\gamma2$ receptors are generally reduced for all the agonists (Table 3; Supplemental Fig. 3*A–C*). This caused either a decrease or no change in the agonist dissociation constants for monoliganded receptors (K_1) whilst K_2 (for

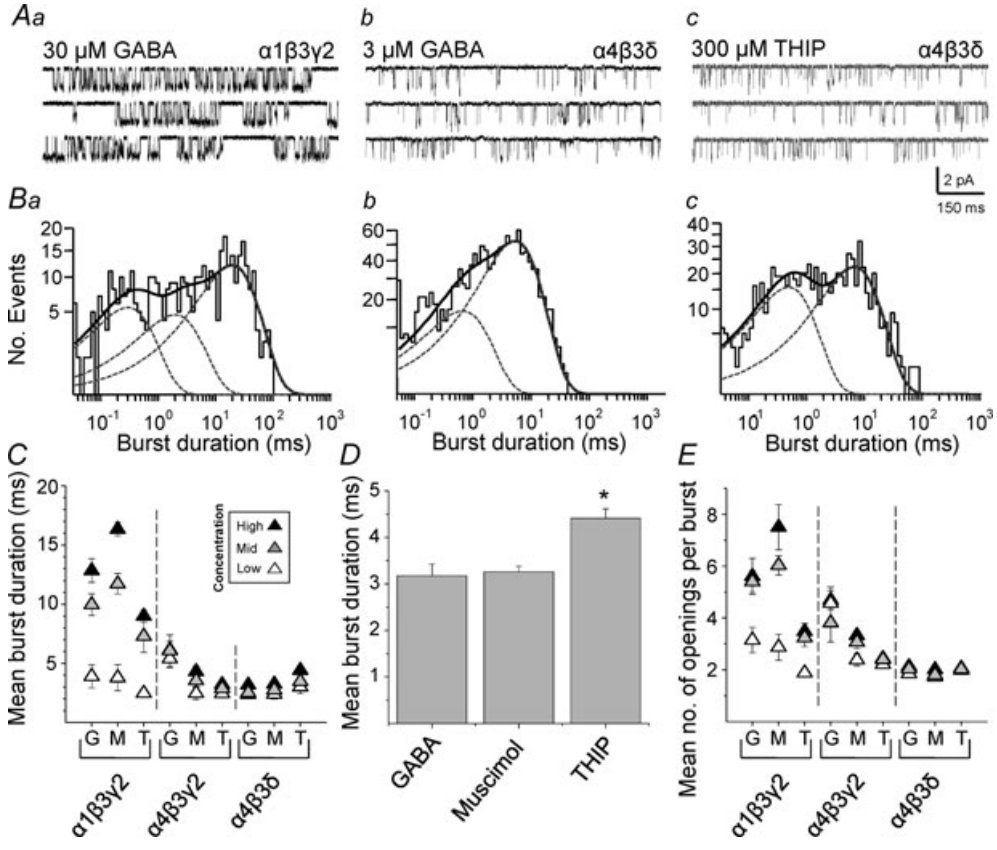

Figure 7. Channel burst analysis for synaptic- and extrasynaptic-type $GABA_A$ receptors
A, sample single channel recordings of bursts and single open events induced by GABA (30 μM) on $\alpha1\beta3\gamma2$ (*a*), GABA (3 μM) on $\alpha4\beta3\delta$ (*b*), and THIP (300 μM) on $\alpha4\beta3\delta$ (*c*). *B*, burst duration distributions corresponding to the receptor isoforms shown in (*A*). Individual (dotted lines) and summed exponential fits (continuous line) are shown. *C*, mean burst durations for GABA (G), muscimol (M) and THIP (T) for three concentrations at each receptor isoform. *D*, bar graph of the mean burst durations for $\alpha4\beta3\delta$ $GABA_A$ receptors with the highest concentrations of GABA, muscimol and THIP (*$P = 0.0005$, ANOVA, $n = 6–7$). *E*, mean number of openings per burst for three concentrations of GABA, muscimol and THIP on each receptor isoform. $n = 5–7$.

Table 3. Rate constants for transitions between states of $\alpha1\beta3\gamma2$, $\alpha4\beta3\gamma2$ and $\alpha4\beta3\delta$ $GABA_A$ receptors activated by GABA, muscimol and THIP

		$\alpha1\beta3\gamma2$			$\alpha4\beta3\gamma2$			$\alpha4\beta3\delta$		
Constant	Unit	GABA	Muscimol	THIP	GABA	Muscimol	THIP	GABA	Muscimol	THIP
k_1	$M^{-1} * s^{-1}$	51×10^6	453×10^6	1.6×10^6	3.5×10^6	7.1×10^6	3.9×10^6	32×10^6	15×10^6	5.7×10^6
k_{-1}	s^{-1}	399	245	3	6	6	6	7	1.3	56
k_2	$M^{-1} * s^{-1}$	28×10^6	186×10^6	2.6×10^6	3.2×10^6	5.9×10^6	0.8×10^6	47×10^6	21×10^6	0.15×10^6
k_{-2}	s^{-1}	360	428	842	51	28	285	12	7	53
δ	s^{-1}	219	217	110	2	5	6	6	6	7
δ_{-1}	s^{-1}	17	21	15	3	11	15	3	6	2
β_1	s^{-1}	570	427	40	57	45	39	20	22	142
α_1	s^{-1}	2268	2471	2695	2972	2887	1625	465	1324	956
β_2	s^{-1}	2556	2690	1543	936	887	676	255	325	1362
α_2	s^{-1}	356	324	394	970	1023	812	1500	1729	348
K_1	μM	7.9	0.5	1.7	1.8	0.8	1.5	0.2	0.1	9.8
K_2	μM	12.8	2.3	330	16.0	4.7	357	0.3	0.3	359
D		13	10	7	0.62	0.45	0.40	2.0	1.0	3.5
E_1		0.25	0.17	0.01	0.019	0.016	0.024	0.04	0.02	0.15
E_2		7.2	8.3	3.9	1.0	0.9	0.8	0.17	0.19	3.9

The rate constants were determined by optimally fitting the single channel data for each receptor ($\alpha1\beta3\gamma2$, $\alpha4\beta3\gamma2$ and $\alpha4\beta3\delta$) in the presence of each agonist (GABA, muscimol and THIP) at each of the three concentrations with the linear/branched receptor model using QuB. Values are accrued from $n = 13$–20 patches.

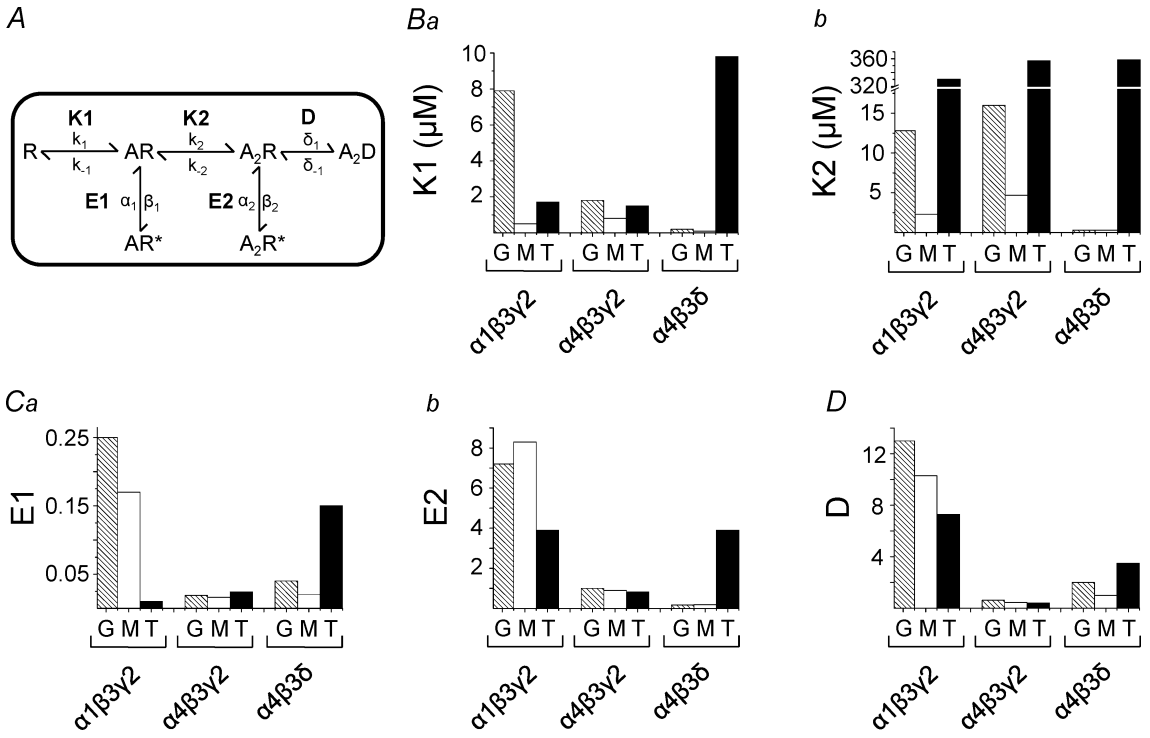

Figure 8. Binding and conformation constants for GABA, muscimol and THIP for synaptic- and extrasynaptic-type receptors

These constants were determined from the single channel rate constants determined from fitting the linear/branched model to the single channel data for all three receptors: $\alpha1\beta3\gamma2$, $\alpha4\beta3\gamma2$ and $\alpha4\beta3\delta$ receptors. *A*, $GABA_A$ receptor kinetic model. *B*, dissociation constants for monoliganded (K_1; *a*) and bilganded (K_2; *b*) receptor states. *C*, efficacies for the monoliganded (E_1; *a*) and bilganded (E_2;*b*) gating transitions. *D*, desensitisation equilibrium constants (*D*) calculated for GABA, muscimol and THIP.

biliganded receptors) was generally increased for each agonist (Fig. 8*B*). As for $\alpha1\beta3\gamma2$ receptors, THIP exhibited the highest value for K_2 compared to GABA and muscimol. With regard to channel gating, generally, β was lower and α was higher for $\alpha4\beta3\gamma2$ compared to $\alpha1\beta3\gamma2$ with little distinction between the agonists (Table 3; Supplemental Fig. 3*Ac–Cc*). Consequently, agonist efficacy for the biliganded $\alpha4\beta3\gamma2$ receptor (E_2) was less than 1 and much smaller compared with E_2 for $\alpha1\beta3\gamma2$ (Table 3; Fig. 8*Cb*). Finally, the entry and exit from desensitisation was also noticeably slower for $\alpha4\beta3\gamma2$ compared to $\alpha1\beta3\gamma2$ receptors such that D (δ_1/δ_{-1}) was less than 1 (Fig. 8*D*).

We next considered the consequences for the model rate constants by exchanging the $\gamma2$ subunit for δ forming the $\alpha4\beta3\delta$ receptor (Supplemental Fig. 4). The forward binding rate constant (k_1) for GABA is similar to that for the $\alpha1\beta3\gamma2$ receptor, whilst for muscimol the binding rate is reduced. By comparison, the unbinding rate constants (k_{-1}) are smaller, causing K_1 and K_2 to be substantially reduced (Table 3; Fig. 8*B*) contributing to the leftward displacement of the GABA and muscimol concentration–response curves (Fig. 1*Bc*).

However, for THIP, the binding rates are slower but the unbinding is much faster causing K_1 and K_2 to be much larger compared to values for GABA and muscimol (Fig. 8*B*). Thus, the concentration–response curve is displaced to higher concentrations as observed (Fig. 1*Bc*). Despite the differential binding rates to $\alpha4\beta3\delta$ receptors, the most significant difference between the agonists concerns the gating of the channel. Here the opening rate (β) is far higher for THIP for both mono-liganded and bilganded receptors, and generally, the closing rate (α) is also slower (Table 3). This significantly increases E_1 and E_2 for THIP compared with the efficacies for either GABA or muscimol (Fig. 8*C*; Supplemental Fig. 4).

As noted for the $\alpha4\beta3\gamma2$ receptor, the entry into and exit from desensitisation for $\alpha4\beta3\delta$ receptors are again slow for all the agonists. The estimates of D are slightly higher than for $\alpha4\beta3\gamma2$, but much less than for $\alpha1\beta3\gamma2$ receptors (Fig. 8*D*). Interestingly, THIP caused greater desensitisation of these extrasynaptic-type receptors than either GABA or muscimol. Although direct comparisons are difficult, the similarity is striking between the single channel predictions for the dissociation constants for THIP (particularly K_2), its efficacy (E_1 and E_2) and its ability to desensitise (D) the $\alpha4\beta3\delta$ receptors compared with the estimated constants, K, E and D, determined from the whole-cell concentration–response curve fits (Fig. 1*B*; Table 2).

Finally, we determined the adequacy of the rate constants, determined from our single channel records, to account for the behaviour of the three agonists at each receptor isoform. This was accomplished by using the rate constants to predict the peak current amplitudes that would be apparent following the activation of $\alpha1\beta3\gamma2$, $\alpha4\beta3\gamma2$ and $\alpha4\beta3\delta$ receptors with a concentration range for each agonist. The adequacy of our receptor model was then assessed by constructing theoretical agonist concentration–response curves entirely from the single channel data (Fig. 9). These curves accurately reproduced the concentration–response curves generated from the whole-cell current data (Fig. 1) including the lower potency of THIP at all three receptors, the higher potency of muscimol compared to GABA, and, of importance, the superagonist effect of THIP, and of muscimol, on the $\alpha4\beta3\delta$ receptors (Fig. 9*C*).

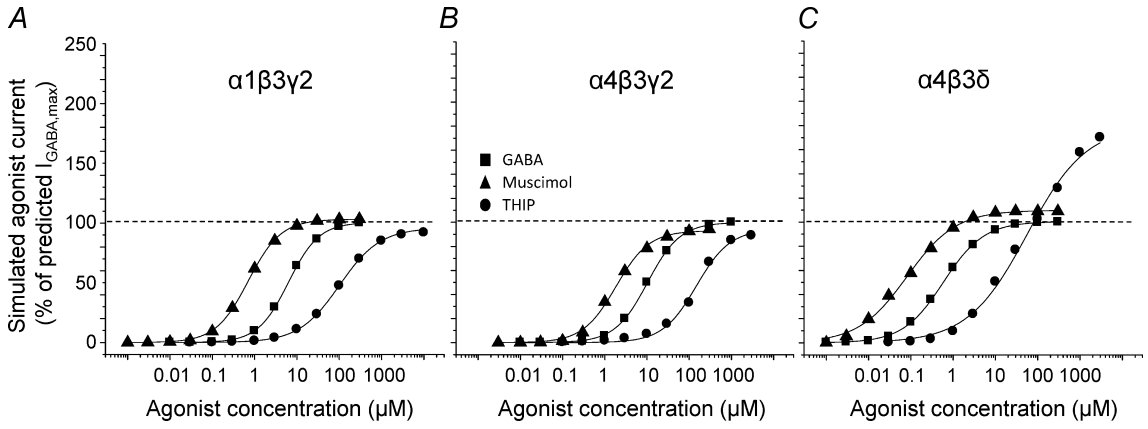

Figure 9. Theoretical whole-cell agonist concentration–response curves
The curves were generated from the state function for the linear/branched receptor model. The transition constants in the model were determined from the single channel rate constants following the predictive fitting of the single channel data with the linear/branched receptor model using QuB. The data points represent the peaks of simulated currents that were subsequently generated in ChanneLab using the linear/branched model and the best fit single channel rate constants for each agonist. Simulated concentration–response curves for GABA (squares), muscimol (triangles) and THIP (circles) are shown for $\alpha1\beta3\gamma2$ (*A*), $\alpha4\beta3\gamma2$ (*B*) and $\alpha4\beta3\delta$ (*C*) $GABA_A$ receptors.

Discussion

This study examined the biophysical properties of typical synaptic- ($\alpha1\beta3\gamma2$) and extrasynaptic-type ($\alpha4\beta3\delta$) $GABA_A$ receptors plus $\alpha4\beta3\gamma2$, whose cellular location is less certain, by using three agonists that are known to have distinct effects: the natural transmitter GABA, the potent agonist muscimol, and THIP, which displays superagonist behaviour at δ subunit-containing receptors.

Agonist potency at synaptic and extrasynaptic-type receptors

The order of potency for the agonists is independent of the $GABA_A$ receptor subunit composition studied here, with muscimol > GABA >> THIP. Agonist potencies (EC_{50} values) were increased by 25–38% after replacing $\alpha1$ with $\alpha4$ subunits in $\alpha\beta3\gamma2$ receptors; and further increased by 78–90% after exchanging $\gamma2$ for the δ subunit in $\alpha4\beta3\delta$ receptors. Increased agonist potency has been noted previously with $\alpha4$ and δ subunit-containing $GABA_A$ receptors (Whittemore *et al.* 1996; Brown *et al.* 2002), although others report no difference (Wafford *et al.* 1996; Lagrange *et al.* 2007). A major contributory factor affecting potency at synaptic- and extrasynaptic-type receptors is the agonist dissociation constant (K), which for the biliganded receptors (K_2), has the following order: THIP > GABA > muscimol. The potency of agonists can be affected by their efficacies (E; Supplemental Fig. 5*A*), but for $\alpha4\beta3\gamma2$ and $\alpha4\beta3\delta$, E_1 and E_2 for GABA and muscimol are much lower than corresponding values for $\alpha1\beta3\gamma2$ receptors, which would tend to lower the potency, contrary to what we observed. Thus, the agonist dissociation constant rather than efficacy seems to dominate the potency rank order. Nevertheless, increased efficacy (E_1 and E_2) may contribute to the increased potency for THIP at $\alpha4\beta3\delta$ compared to $\alpha1\beta2\gamma2$ receptors. THIP's conformationally constrained double ring structure underlies its partial agonist behaviour at most synaptic-type $\alpha\beta\gamma$ $GABA_A$ receptors due to a suboptimal fit at the binding site compared with the more flexible GABA molecule (Krogsgaard-Larsen, 1988). However, this does not appear to be significant for $\alpha4\beta3\delta$ receptors, where the increased potency depends on a domain in the δ subunit, stretching from M1 through the M1–M2 linker and just into M2 (You & Dunn, 2007).

Our results concur with the notion that synaptic $\gamma2$ subunit-containing receptors ($\alpha1\beta3\gamma2$) are less sensitive to agonists than their extrasynaptic counterparts ($\alpha4\beta3\delta$). Native receptors will also experience different GABA concentrations. At synapses, receptors are briefly exposed to low millimolar concentrations following phasic GABA release, whilst extrasynaptic receptors experience an ambient overspill from synapses attaining 0.2–2 μM GABA (Stell & Mody, 2002; Caraiscos *et al.* 2004; Mortensen & Smart, 2006; Mtchedlishvili & Kapur, 2006).

Although $\alpha1\beta3\gamma2$ receptors showed significant desensitisation, our single channel recordings suggested this was not so apparent for $\alpha4\beta3\gamma2$ receptors. Previously, $\alpha4$ subunit-containing receptors have been reported to desensitise either more slowly (Picton & Fisher, 2007) or more rapidly (Lagrange *et al.* 2007) compared to $\alpha1$ subunit-containing receptors. As we could only accurately assess closed times within bursts we would have missed long desensitised periods in our channel analyses leading to an underestimation of the degree of desensitisation for $\alpha4$ receptors. Replacing the $\gamma2$ subunit with δ in the $\alpha4\beta3\delta$ receptors reintroduced desensitisation in our single channel experiments. This was surprising given that extrasynaptic GABA receptors containing the δ subunit (e.g. $\alpha1\beta3\delta$) are considered to desensitise at a slow rate (Haas & MacDonald, 1999; Bianchi *et al.* 2001; Bianchi *et al.* 2001). The model rate constants determined for the $\alpha4\beta3\delta$ receptor suggested that at low agonist concentrations ($<1\,\mu$M), the receptor could already be partly desensitised. Simulating agonist-activated currents for GABA ($0.3\,\mu$M) and muscimol ($0.3\,\mu$M) indicated the level of desensitisation can be considerable (Fig. 10). Thus, from this study, we would predict that the extrasynaptic $\alpha4\beta3\delta$ receptor population that supports tonic inhibition, which is exposed to low submicromolar basal concentrations of GABA, will be substantially desensitised.

Examination of the whole-cell current decays during agonist application did reveal the prospect of multiple phases of desensitisation. In our receptor model, the state 'D' represents a composite state that may include more than one discrete desensitised state. The reason for choosing this approach is that our single channel cluster analyses will mostly reflect only rapid desensitised states. The long desensitised periods that typify the longer tails of the whole-cell currents are better correlated with long closed periods between channel clusters; however, these inter-cluster closures may become contaminated by the appearance of more than one channel in the patch. Finally, we employed extended branching of the receptor model to include additional D states, but this did not improve the quality of the data fits. For these reasons a composite D state was preferred.

A consistent feature with all three receptors was the rapid deactivation observed with THIP induced currents, contrasting with the slowly deactivating muscimol currents, a difference also noted for these agonists activating $\alpha1\beta1\gamma2$ receptors (Bianchi *et al.* 2007). This characteristic is likely to depend principally on agonist dissociation from the receptor and our results demonstrate that this is generally more rapid for THIP compared to GABA and muscimol at all three receptors.

Low pH can increase GABA channel current

The superagonist activity of THIP could arise from an increase in the channel current and/or modulation of channel kinetics. Our single channel recordings demonstrated that THIP does not affect the single channel current. Nevertheless, an increased conductance has been reported for $\alpha1\beta2\gamma2$ and $\alpha4\beta2\gamma2$ receptors, but only with saturating THIP concentrations (10 mM) (Keramidas & Harrison, 2008). Significantly, the increased channel conductance was evident for both $\gamma2$ and δ subunit-containing receptors. Alone, this would not account for the superagonist effect of THIP at $\alpha4\beta\delta$ receptors, but is it likely to be a contributory factor? We can emulate the increased conductance by THIP, but only by allowing the 10 mM THIP solution to remain acidified at pH 4. This will significantly increase the cationic form of THIP (Krogsgaard-Larsen *et al.* 1994) at the expense of its zwitterion and could conceivably affect THIP's orientation at the ligand binding site, altering transduction and increasing channel conductance. An increased channel conductance was also induced by GABA, at pH 4, where its cationic form predominates (Krishek *et al.* 1996). Thus, a change in conductance is unlikely to contribute to THIP's unusual superagonist behaviour. Interestingly, previous studies of neuronal $GABA_A$ receptor channels have not observed an increased channel conductance at acidic pH (Huang & Dillon, 1999; Krishek & Smart, 2001), but the highest concentration of protons examined was only 2.5 μM (pH 5.6) compared to the 100 μM achieved at pH 4.

High efficacy superagonist behaviour of THIP

The constant nature of the single channel current indicates that THIP's superagonist activity must reside in the kinetic properties associated with δ subunit-containing receptors. The $\alpha4$ subunit is probably not important for superagonism since THIP did not display this activity at $\alpha4\beta3\gamma2$ receptors. Superagonism might originate from the agonist binding site, but the δ subunit is considered an unlikely component for binding, since the agonist site resides at the β–α subunit interface (Sigel *et al.* 1992; Amin & Weiss, 1993; Wagner & Czajkowski, 2001; Baumann *et al.* 2003; Wagner *et al.* 2004). However, co-expression of subunit-constrained $GABA_A$ receptors, using $\alpha1$–$\beta3$–$\alpha1$ and $\beta3$–δ concatamers, suggested that the δ-subunit may contribute to or affect the agonist binding site (Kaur *et al.* 2009), a feature that could then influence THIP activation of $\alpha\beta\delta$ receptors. Nevertheless, the low potency of THIP compared to GABA and muscimol suggested that an alternative explanation of superagonism is required which does not involve ligand binding and probably derives from altered signal transduction from the binding site to the channel.

A comparison of the activation profiles of the three receptors proved instructive. Agonist activation of $\alpha1\beta3\gamma2$ receptors produced channel openings with longer mean open times and longer bursts of channel activity, containing on average more openings per burst, resulting in higher open probabilities. By comparison, $\alpha4\beta3\gamma2$ and $\alpha4\beta3\delta$ receptors were compromised in terms of mean open times, the mean number of openings per burst, and therefore their mean burst durations. Notably, long bursts and the presence of clusters were far less prominent with $\alpha4$ subunit-containing receptors, a feature noted previously for $\alpha4\beta2\gamma2$ receptors (Akk *et al.* 2004). For the superagonist activity of THIP on $\alpha4\beta3\delta$ $GABA_A$ receptors, the most important change was the increase in the long open time (τ_{O2}) by high concentrations of THIP, when compared with high concentrations of GABA and muscimol. By contrast, the mean number of openings per

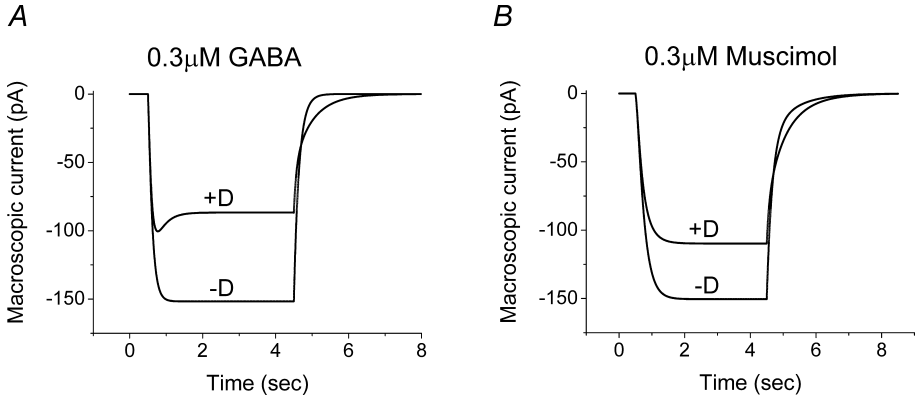

Figure 10. Extrasynaptic-type $\alpha4\beta3\delta$ receptors are desensitised by low GABA concentrations
Simulated agonist-activated currents are presented for the linear/branched receptor model. The transition constants used in the model to generate the currents were determined after predictive fitting of the single channel data for GABA and muscimol. Two simulations were used; one in which access to the desensitised state (D) was allowed (+D state) and one in which desensitisation was absent (–D state). Notably, the receptor is substantially desensitised by low concentrations of GABA (*A*) or muscimol (*B*) that do not cause overt fading of the current response.

burst was similar for the three agonists on $\alpha4\beta3\delta$ receptors, so the longer burst durations caused by THIP must follow the induction of longer mean open times. Using our kinetic model, THIP substantially increased both E_1 and E_2 at $\alpha4\beta3\delta$ receptors and this is the fundamental reason for its superagonist behaviour even though THIP has low potency and caused more desensitisation of these receptors.

Whilst the superagonist activity of THIP at $\alpha4\beta3\delta$ receptors (Adkins *et al.* 2001; Brown *et al.* 2002) can be largely ascribed to increased efficacy, this does not explain the superagonist behaviour displayed by muscimol (Storustovu & Ebert, 2006). Muscimol has much lower dissociation constants at $\alpha4\beta3\delta$ receptors compared to THIP and thus will bind more tightly, but this also does not explain its superagonist behaviour. Indeed, our model predicts that muscimol's efficacy at $\alpha4\beta3\delta$ receptors is lower than that for THIP and on a par with that for GABA (E_2) or even lower (E_1). Therefore, the only plausible explanation for muscimol's superagonist activity is that it causes less desensitisation at $\alpha4\beta3\delta$ receptors compared to both GABA and THIP. Reducing the conformational constant D in the model would manifest as an increase in apparent efficacy (Supplemental Fig. 5*B*) by scaling the concentration–response curve but without causing any shift in agonist potency, unlike changes to E.

In conclusion, the potency of the agonists at the three receptor isoforms is largely determined by their dissociation constants, and thus is a function of agonist binding. In comparison, the superagonist behaviour of THIP results from increased efficacy at extrasynaptic receptors whilst the superagonist behaviour of muscimol relies on reduced desensitisation of extrasynaptic receptors. Thus, there are two principle mechanisms for promoting superagonist behaviour at extrasynaptic receptors and this ability to selectively increase the efficacy and/or reduce the desensitisation of extrasynaptic $GABA_A$ receptor activation may prove to be a useful therapeutic avenue under circumstances when synaptic inhibition becomes dysfunctional.

References

Adkins CE, Pillai GV, Kerby J, Bonnert TP, Haldon C, McKernan RM, Gonzalez JE, Oades K, Whiting PJ & Simpson PB (2001). $\alpha4\beta3\delta$ $GABA_A$ receptors characterized by fluorescence resonance energy transfer-derived measurements of membrane potential. *J Biol Chem* **276**, 38934–38939.

Akk G, Bracamontes J & Steinbach JH (2004). Activation of $GABA_A$ receptors containing the $\alpha4$ subunit by GABA and pentobarbital. *J Physiol* **556**, 387–399.

Amin J & Weiss DS (1993). $GABA_A$ receptor needs two homologous domains of the β-subunit for activation by GABA but not by pentobarbital. *Nature* **366**, 565–569.

Banks MI & Pearce RA (2000). Kinetic differences between synaptic and extrasynaptic $GABA_A$ receptors in CA1 pyramidal cells. *J Neurosci* **20**, 937–948.

Baumann SW, Baur R & Sigel E (2003). Individual properties of the two functional agonist sites in $GABA_A$ receptors. *J Neurosci* **23**, 11158–11166.

Bianchi MT, Haas KF & MacDonald RL (2001). Structural determinants of fast desensitization and desensitization-deactivation coupling in $GABA_A$ receptors. *J Neurosci* **21**, 1127–1136.

Bianchi MT, Botzolakis EJ, Haas KF, Fisher JL & Macdonald RL (2007). Microscopic kinetic determinants of macroscopic currents: insights from coupling and uncoupling of $GABA_A$ receptor desensitization and deactivation. *J Physiol* **584**, 769–787.

Brown N, Kerby J, Bonnert TP, Whiting PJ & Wafford KA (2002). Pharmacological characterization of a novel cell line expressing human $\alpha4\beta3\delta$ $GABA_A$ receptors. *Br J Pharmacol* **136**, 965–974.

Burzomato V, Beato M, Groot-Kormelink PJ, Colquhoun D & Sivilotti LG (2004). Single-channel behaviour of heteromeric $\alpha1\beta$ glycine receptors: an attempt to detect a conformational change before the channel opens. *J Neurosci* **24**, 10924–10940.

Caraiscos VB, Elliott EM, You T, Cheng VY, Belelli D, Newell JG, Jackson MF, Lambert JJ, Rosahl TW, Wafford KA, MacDonald JF & Orser BA (2004). Tonic inhibition in mouse hippocampal CA1 pyramidal neurons is mediated by $\alpha5$ subunit-containing γ-aminobutyric acid type A receptors. *Proc Natl Acad Sci U S A* **101**, 3662–3667.

Colquhoun D & Sakmann B (1985). Fast events in single-channel currents activated by acetylcholine and its analogues at the frog muscle end-plate. *J Physiol* **369**, 501–557.

Ebert B, Wafford KA, Whiting PJ, Krogsgaard-Larsen P & Kemp JA (1994). Molecular pharmacology of γ-aminobutyric acid type A receptor agonists and partial agonists in oocytes injected with different α, β, and γ receptor subunit combinations. *Mol Pharmacol* **46**, 957–963.

Fischer F, Kneussel M, Tintrup H, Haverkamp S, Rauen T, Betz H & Wassle H (2000). Reduced synaptic clustering of GABA and glycine receptors in the retina of the gephyrin null mutant mouse. *J Comp Neurol* **427**, 634–648.

Fritschy JM & Brunig I (2003). Formation and plasticity of GABAergic synapses: physiological mechanisms and pathophysiological implications. *Pharmacol Ther* **98**, 299–323.

Gingrich KJ, Roberts WA & Kass RS (1995). Dependence of the $GABA_A$ receptor gating kinetics on the α-subunit isoform: implications for structure-function relations and synaptic transmission. *J Physiol* **489**, 529–543.

Haas KF & MacDonald RL (1999). $GABA_A$ receptor subunit $\gamma2$ and δ subtypes confer unique kinetic properties on recombinant $GABA_A$ receptor currents in mouse fibroblasts. *J Physiol* **514**, 27–45.

Hadingham KL, Harkness PC, McKernan RM, Quirk K, Le Bourdelles B, Horne AL, Kemp JA, Barnard EA, Ragan CI & Whiting PJ (1992). Stable expression of mammalian type A γ-aminobutyric acid receptors in mouse cells: Demonstration of functional assembly of benzodiazepine-responsive sites. *Proc Natl Acad Sci U S A* **89**, 6378–6382.

Hatton CJ, Shelley C, Brydson M, Beeson D & Colquhoun D (2003). Properties of the human muscle nicotinic receptor, and of the slow-channel myasthenic syndrome mutant εL221F, inferred from maximum likelihood fits. *J Physiol* **547**, 729–760.

Huang RQ & Dillon GH (1999). Effect of extracellular pH on GABA-activated current in rat recombinant receptors and thin hypothalamic slices. *J Neurophysiol* **82**, 1233–1243.

Jones MV & Westbrook GL (1995). Desensitized states prolong $GABA_A$ channel responses to brief agonist pulses. *Neuron* **15**, 181–191.

Kaur KH, Baur R & Sigel E (2009). Unanticipated structural and functional properties of δ-subunit-containing $GABA_A$ receptors. *J Biol Chem* **284**, 7889–7896.

Keramidas A & Harrison NL (2008). Agonist-dependent single channel current and gating in $\alpha4\beta2\delta$ and $\alpha1\beta2\gamma2$S $GABA_A$ receptors. *J Gen Physiol* **131**, 163–181.

Keramidas A & Harrison NL (2009). The activation mechanism of $\alpha1\beta2\gamma2$S and $\alpha3\beta3\gamma2$S $GABA_A$ receptors. *J Gen Physiol* **135**, 59–75.

Krishek BJ, Amato A, Connolly CN, Moss SJ & Smart TG (1996). Proton sensitivity of the $GABA_A$ receptor is associated with the receptor subunit composition. *J Physiol* **492**, 431–443.

Krishek BJ & Smart TG (2001). Proton sensitivity of rat cerebellar granule cell $GABA_A$ receptors: dependence on neuronal development. *J Physiol* **530**, 219–233.

Krogsgaard-Larsen P (1988). GABA synaptic mechanisms: stereochemical and conformational requirements. *Med Res Rev* **8**, 27–56.

Krogsgaard-Larsen P, Frolund B, Jorgensen FS & Schousboe A (1994). $GABA_A$ receptor agonists, partial agonists, and antagonists: Design and therapeutic prospects. *J Med Chem* **37**, 2489–2505.

Krogsgaard-Larsen P, Frolund B & Liljefors T (2002). Specific $GABA_A$ agonists and partial agonists. *Chem Rec* **2**, 419–430.

Krogsgaard-Larsen P, Johnston GA, Lodge D & Curtis DR (1977). A new class of GABA agonist. *Nature* **268**, 53–55.

Lagrange AH, Botzolakis EJ & Macdonald RL (2007). Enhanced macroscopic desensitization shapes the response of $\alpha4$ subtype-containing $GABA_A$ receptors to synaptic and extrasynaptic GABA. *J Physiol* **578**, 655–676.

Luscher B & Keller CA (2004). Regulation of $GABA_A$ receptor trafficking, channel activity, and functional plasticity of inhibitory synapses. *Pharmacol Ther* **102**, 195–221.

Matsuda K, Hosie AM, Buckingham SD, Squire MD, Baylis HA & Sattelle DB (1996). pH-dependent actions of THIP and ZAPA on an ionotropic *Drosophila melanogaster* GABA receptor. *Brain Res* **739**, 335–338.

Mortensen M, Kristiansen U, Ebert B, Frolund B, Krogsgaard-Larsen P & Smart TG (2004). Activation of single heteromeric $GABA_A$ receptor ion channels by full and partial agonists. *J Physiol* **557**, 389–413.

Mortensen M & Smart TG (2006). Extrasynaptic α subunit $GABA_A$ receptors on rat hippocampal pyramidal neurons. *J Physiol* **577**, 841–856.

Mortensen M & Smart TG (2007). Single-channel recording of ligand-gated ion channels. *Nat Protocols* **2**, 2826–2841.

Mtchedlishvili Z & Kapur J (2006). High-affinity, slowly desensitizing $GABA_A$ receptors mediate tonic inhibition in hippocampal dentate granule cells. *Mol Pharmacol* **69**, 564–575.

Picton AJ & Fisher JL (2007). Effect of the α subunit subtype on the macroscopic kinetic properties of recombinant $GABA_A$ receptors. *Brain Res* **1165**, 40–49.

Qin F (2004). Restoration of single-channel currents using the segmental k-means method based on hidden Markov modelling. *Biophys J* **86**, 1488–1501.

Qin F, Auerbach A & Sachs F (1996). Estimating single-channel kinetic parameters from idealized patch-clamp data containing missed events. *Biophys J* **70**, 264–280.

Sieghart W & Sperk G (2002). Subunit composition, distribution and function of $GABA_A$ receptor subtypes. *Curr Top Med Chem* **2**, 795–816.

Sigel E, Baur R, Kellenberger S & Malherbe P (1992). Point mutations affecting antagonist affinity and agonist dependent gating of $GABA_A$ receptor channels. *EMBO J* **11**, 2017–2023.

Stell BM & Mody I (2002). Receptors with different affinities mediate phasic and tonic $GABA_A$ conductances in hippocampal neurons. *J Neurosci* **22**, RC223.

Storustovu S & Ebert B (2006). Pharmacological characterization of agonists at δ-containing $GABA_A$ receptors: functional selectivity for extrasynaptic receptors is dependent on the absence of $\gamma2$. *J Pharmacol Exp Ther* **316**, 1351–1359.

Sur C, Farrar SJ, Kerby J, Whiting PJ, Atack JR & McKernan RM (1999). Preferential coassembly of $\alpha4$ and δ subunits of the γ-aminobutyric $acid_A$ receptor in rat thalamus. *Mol Pharmacol* **56**, 110–115.

Wafford KA, Thompson SA, Thomas D, Sikela J, Wilcox AS & Whiting PJ (1996). Functional characterization of human γ-aminobutyric $acid_A$ receptors containing the $\alpha4$ subunit. *Mol Pharmacol* **50**, 670–678.

Wagner DA & Czajkowski C (2001). Structure and dynamics of the GABA binding pocket: a narrowing cleft that constricts during activation. *J Neurosci* **21**, 67–74.

Wagner DA, Czajkowski C & Jones MV (2004). An arginine involved in GABA binding and unbinding but not gating of the $GABA_A$ receptor. *J Neurosci* **24**, 2733–2741.

Whittemore ER, Yang W, Drewe JA & Woodward RM (1996). Pharmacology of the human γ-aminobutyric $acid_A$ receptor $\alpha4$ subunit expressed in *Xenopus laevis* oocytes. *Mol Pharmacol* **50**, 1364–1375.

Wisden W, Laurie DJ, Monyer H & Seeburg PH (1992). The distribution of 13 $GABA_A$ receptor subunit mRNAs in the rat brain. I. Telencephalon, diencephalon, mesencephalon. *J Neurosci* **12**, 1040–1062.

Yeung JY, Canning KJ, Zhu G, Pennefather P, MacDonald JF & Orser BA (2003). Tonically activated $GABA_A$ receptors in hippocampal neurons are high-affinity, low-conductance sensors for extracellular GABA. *Mol Pharmacol* **63**, 2–8.

You H & Dunn SM (2007). Identification of a domain in the subunit (S238-V264) of the $\alpha4\beta3\delta$ $GABA_A$ receptor that confers high agonist sensitivity. *J Neurochem* **103**, 1092–1101.

Author contributions

All authors contributed to the conception and design of the experiments. Data collection, analysis, interpretation and writing the paper was carried out by M.M. and T.G.S. All authors revised and approved of the final version of the manuscript.

Acknowledgements

This work was supported by the MRC. We are grateful to Damian Bright and Philip Thomas for helpful comments on the manuscript.